

https://doi.org/10.1070/QEL17281

Phase-shift speckle-shearing interferometry

G.N. Vishnyakov, A.D. Ivanov, G.G. Levin, V.L. Minaev

Abstract. **We have numerically simulated the process of measuring stress–strain states by the method of speckle-shearing interferometry using the phase-shift technique. A computer model with the possibility of setting its strain and roughness is developed, which includes a model of a diffusely reflecting test object corresponding to the characteristics of a real membrane, as well as a speckle interferometer model that allows speckle interferograms to be obtained for different speckle sizes and angles between interfering beams. The process of reconstructing the object surface topogram from model speckle interferograms by the phase-shift technique is implemented. Using the developed models, a two-dimensional shearogram are obtained, which is a derivative of the strain field of a circular membrane. Comparison of the results of numerical simulation with experimental data shows that the differences (rms deviations) do not exceed 0.02 μm. It is also shown that the error of interferogram reconstruction by the phase-shift technique increases significantly when the test object strains exceed 12 μm.**

Keywords: *speckle interferometry, schearography, phase-shift technique, stress–strain states, simulation.*

1. Introduction

Methods of digital or electronic speckle interferometry are widely used for non-destructive testing in various production areas, for example, in the aerospace industry and mechanical engineering, where composite materials and products of additive technologies are actively used [1]. Using this non-contact method, micro-displacements of individual parts of the product's surface are studied during their deformation under various types of loads (mechanical, thermal, etc.).

One of the varieties of speckle interferometry is speckle-shearing interferometry, or schearography [2, 3]. This method uses the interference of two speckle fields shifted relative to each other. Shearographs belong to the class of interferometers with combined object and reference beams, or, in other words, to the so-called common-path interferometers. In such interferometers, the reference beam is formed from the object beam. This implies an important property of speckle-shearing interferometry, i.e. low sensitivity to object vibrations, which allows shearography in real production conditions, without any protection from vibrations.

To obtain quantitative information about an object, various methods of phase reconstruction from interferograms should be used. The decoding of speckle interferograms is performed by the methods being traditional for modern interferometry, which are usually divided into two categories in digital shearography: temporal phase-shift digital shearography (TPS-DS) and spatial phase-shift digital shearography (SPS-DS) [4]. The temporal phase-shift method has a higher accuracy of phase reconstruction from interferograms [4], and so we will use it in this work. The reconstructed phase image is related to the derivative of the displacement field in the displacement direction, i.e., with the displacement field gradient.

In the practical implementation of phase-shift speckle-shearing interferometry, some questions arise that can only be answered after preliminary mathematical simulation. Thus, of importance is the choice of an algorithm for sequential processing of speckle interferograms, a method for filtering an intermediate result of reconstruction in the form of a 'wrapped' phase, etc. The development of a mathematical model of a shearograph will allow one to establish the limits of the method applicability and evaluate the measurement errors, and in addition, to reveal the dependences of the reconstruction result on the object characteristics. Simulating the speckle interferometer's optical system will also allow one to find its optimal parameters. The development of a computer model of a test-object is necessary to verify the operation of the phase reconstruction algorithm and subsequent computer simulation of the process of measuring the stress–strain states by shearography. Computer simulation of the shearogram makes it possible to pre-set the desired value of the image shift in the optical scheme to obtain the predictable result and measurement error when adjusting and tuning the device. This approach enables us to use a speckle interferometer without a calibration (reference) device.

Thus, the purpose of this work is to develop a computer model for object strain measurements by means of speckle-shearing interferometry with the interferogram decoding using the phase-shift technique, as well as to optimise the algorithm for processing speckle interferograms using the phase-shift method and to compare the results of simulation and experiment.

2. Optical scheme of the shearograph and the equations of shearing interferograms

Various optical schemes are employed to implement speckle-shearing interferometry, but most often use is made of a Michelson interferometer scheme [5]. This is primarily due to

G.N. Vishnyakov All-Russian Research Institute of Optical and Physical Measurements, Ozernaya ul. 46, 119361 Moscow, Russia; Bauman Moscow State Technical University (National Research University), Vtoraya Baumanskaya ul. 5, 105005 Moscow, Russia; e-mail: academi@ya.ru;
A.D. Ivanov, G.G. Levin, V.L. Minaev All-Russian Research Institute of Optical and Physical Measurements, Ozernaya ul. 46, 119361 Moscow, Russia

Received 18 February 2020; revision received 29 March 2020
Kvantovaya Elektronika **50** (7) 636–642 (2020)
Translated by M.A. Monastyrskiy

the simplicity of achieving an image shift by tilting one of the mirrors (mirror – 5 in Fig. 1). Secondly, it is easy to implement quantitative decoding of speckle interferograms in a Michelson interferometer using phase shifting interferometry [1, 2]. Indeed, the essence of this method is to record a set of interferograms with different phase shifts between interfering beams. To form a necessary phase shift, the optical path length of one of the beams changes. This can be done, for example, by micro-displacement along the optical axis of one of the interferometer mirrors mounted on a piezoelectric element (*6*) (Fig. 1).

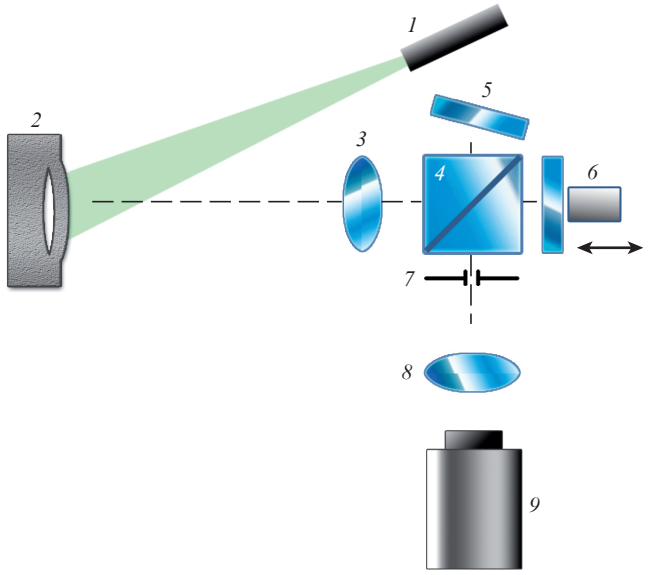

Figure 1. Shearograph based on a Michelson interferometer: (*1*) laser; (*2*) object containing a defect; (*3*) lens; (*4*) beam splitter; (*5*) folding mirror; (*6*) mirror mounted on a piezoelectric actuator; (*7*) diaphragm; (*8*) lens; (*9*) camera.

Two overlapping images of the object are formed on a recorder (*9*), which are shifted relative to each other in the direction transverse to the optical axis. As a recorder (*9*), matrix electronic devices, such as CCD or CMOS cameras, are used. The recorded images are digitised and entered for further digital processing into a computer. Speckle-shearing interferograms before and after loading can be written in the generalised form:

$$I_n(x,y) = a(x,y) + b(x,y)\cos[\Phi_n(x,y)], \tag{1}$$

where a is the amplitude background; n is the visibility of interference fringes; and $n = 1, 2$.

Phase Φ_1 describes the object state before loading and is equal to the phase difference at two adjacent points, x and $x + \Delta x$, divided by the shift value Δx:

$$\Phi_1(x,y) = \varphi(x,y) - \varphi(x + \Delta x, y). \tag{2}$$

Phase Φ_2 describes the object state after loading. It is also equal to the phase difference at points x and $x + \Delta x$, but with the addition of $\Delta\varphi$ caused by the object strain:

$$\Phi_2(x,y) = \varphi(x,y) - \varphi(x + \Delta x, y) + \Delta\varphi(x,y) - \Delta\varphi(x + \Delta x, y). \tag{3}$$

In this work we use the method of five phase shifts proposed in [6] to reconstruct the phase $\Phi_n(x,y)$ from the generalised interferogram (1). The algorithm used to implement this method is resistant to a small 'decalibration' of the phase-shifting device, and, in addition, well suppresses artefacts in the form of the second harmonic. For its implementation, a series of five interferograms with a $\pi/2$ phase shift is recorded:

$$I_n^k(x,y) = a(x,y) + b(x,y)\cos[\Phi_n(x,y) + k\pi/2], \tag{4}$$

where $k = 0, 1, 2, 3, 4$. The reconstructed phase is calculated by the formula [6]

$$\Phi_n(x,y) = \arctan\left[2\frac{I_n^1(x,y) - I_n^3(x,y)}{2I_n^2(x,y) - I_n^4(x,y) - I_n^0(x,y)}\right]. \tag{5}$$

Since the arctan function is defined in the range of $[-\pi, +\pi]$, the so-called 'wrapped phase' is calculated by formula (5), and therefore, the additional operation of 'phase unwrapping' [7] is further required.

In this work, the following image processing sequence is implemented to reconstruct the displacement field gradient from speckle-shearing interferograms:

1. Obtaining five speckle-shearing interferograms according to which the phase image ('wrapped phase') $\Phi_1(x,y)$ in the original (unloaded) state is reconstructed.

2. Obtaining five speckle-shearing interferograms according to which the phase image ('wrapped phase') $\Phi_2(x,y)$ in the loaded state is reconstructed.

3. Subtracting 'wrapped' phase images in the loaded and original states and obtaining a differential 'wrapped' phase image

$$\Delta\Phi(x,y) = |\Phi_1(x,y) - \Phi_2(x,y)| = |\Delta\varphi(x,y) - \Delta\varphi(x + \Delta x, y)|. \tag{6}$$

The 'wrapped' phase image (6) reconstructed from speckle interferograms is, as a rule, very noisy. Therefore, before 'unwrapping' the image, it is necessary to reduce the noise level. The most suitable method for this is sine–cosine filtration in combination with an averaging filter [8]. A good result gives the use of iterative filtering procedure with 20–30 repetitions. Thus, the third step of image processing is sine–cosine filtering.

4. The last stage of processing is the 'unwrapping' of the differential phase image after its filtering and recalculation into the displacement field gradient according to the formula [8]:

$$\Delta\Phi(x,y) = \boldsymbol{k}\frac{\partial \boldsymbol{d}}{\partial x}\Delta x = \left(k_x\frac{\partial u}{\partial x} + k_y\frac{\partial v}{\partial x} + k_x\frac{\partial w}{\partial x}\right)\Delta x, \tag{7}$$

where $\boldsymbol{k} = (k_x, k_y, k_x)$ is the sensitivity vector equal to the difference between the wave vectors of the illuminating beam and the beam reflected from the object; and $\boldsymbol{d} = (u, v, w)$ is the surface displacement vector at the point under study [8, 9].

The measurement sensitivity of the speckle-shearing interferometer can be adjusted by changing the shift value Δx.

3. Simulation of the optical scheme and speckle interferograms of a diffusely scattering test object

At the first stage, the process of forming an interferogram of a diffusely reflecting object for monochromatic (laser) radiation was simulated. This simulation was necessary to clarify the requirements for the roughness parameters of the object (*2*) and the size of the diaphragm (*7*) in the shearograph schematised in Fig. 1, as well as for the angle between the reference and object beams. Simulation and study of speckle fields is an urgent task and is described in a number of papers [10–12].

The field reflected from a diffusely scattering object can be represented in the form of a complex amplitude with phase $\varphi_{\text{rnd}}(x, y)$, which varies randomly according to a uniform law within the interval $[-\pi; +\pi]$ [13]:

$$U_{\text{rnd}}(x, y) = \exp[-\text{i}\varphi_{\text{rnd}}(x, y)]. \tag{8}$$

A circular membrane deformable at the centre and rigidly fixed at the edges was chosen as a computer model of the object. At low loads, the membrane shape can be well approximated by a sphere [14]. Then the field reflected from such a spherical object can be written as follows:

$$U_{\text{mir}}(x, y) = \exp\left[-\text{i}\left(\frac{2\pi m}{R}\sqrt{R^2 - x^2 - y^2}\right)\right], \tag{9}$$

where R is the sphere radius; m is the factor determining the maximum phase incursion on the object (at $m = 1$ the phase incursion is equal to 2π).

Given that the object is diffusely reflective, from (8) and (9) we obtain an expression for the complex amplitude of the field reflected from such an object:

$$U(x, y) = U_{\text{rnd}}(x, y)U_{\text{mir}}(x, y) = \exp\left[-\text{i}\left(\frac{2\pi n}{R}\sqrt{R^2 - x^2 - y^2} + \varphi_{\text{rnd}}(x, y)\right)\right]. \tag{10}$$

To simulate the optical system of a speckle interferometer, we used the classical optical $4f$ system shown in Fig. 2. It contains two confocal Fourier lenses (*2* and *4*) with a diaphragm (*3*) in their common focus. This diaphragm is essentially a low-pass filter that performs spatial filtering of the Fourier spectrum of radiation reflected from the object, which is formed using the first Fourier lens. By changing the diaphragm diameter, it is possible to change the size of speckles in the recording plane. The radiation intensity I in the output plane (*5*), obtained using such a $4f$ system, can be represented by the expression [15]:

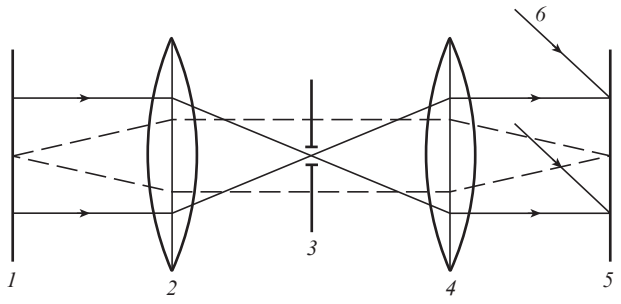

Figure 2. Optical $4f$ system:
(*1*) object plane; (*2*, *4*) Fourier lenses; (*3*) aperture; (*5*) recording plane; (*6*) plane reference beam.

$$I(x, y) = |F^{-1}\{H(x, y)F\{U(x, y)\}\}|^2, \tag{11}$$

where $H(x, y)$ is the coherent transfer function of the optical system, equal to the amplitude transmission of the diaphragm (*3*); and $F\{.\}$ and $F^{-1}\{.\}$ are operators of the direct and inverse Fourier transforms, respectively.

To obtain speckle interferograms, an oblique plane reference wave is used, the complex amplitude of which can be written in the form:

$$r(x, y, k) = \exp[-\text{i}(z(x, y) + k\pi/2)], \tag{12}$$

where $z(x, y)$ is the equation of the incidence plane of the wave; and $k\pi/2$ is the discrete phase shift ($k = 0, 1, 2, 3, 4$), which is required to obtain a series of five speckle interferograms in order to calculate the phase distribution from them using the phase-shift technique.

A speckle interferogram is obtained by quadratic recording of the sum of complex amplitudes of the radiation fields of the object and reference beams:

$$I_{\text{sh}}(x, y, k) = |F^{-1}\{H(x, y)F\{U(x, y)\}\} + r(x, y, k)|^2. \tag{13}$$

By varying the parameter k from 0 to 4, one can obtain a set of five speckle interferograms and reconstruct from them the phase distribution using the phase-shift technique described above. The mathematical model used does not consider the features of light diffraction on a diffusely reflecting surface, depending on the roughness parameters and local slopes of the surface areas. The model extension is the subject of further work on improving the speckle interferogram generation algorithm.

In computer simulation, the test object imitated the membrane deflection and was set in the form of a spherical segment of a certain height (deflection arrow) and the base radius. In this case, the deflection arrow value determined the degree of the membrane strain.

The following geometric parameters of the test object (membrane) were selected for simulation: the image size was 1000×1000 pixels; the base radius was 500 pixels; the deflection arrow was varied in the range 0.1–100 μm and had the values of 0.1, 0.5, 1, 2, 5, 10, 15, 25, 50, 100 μm; and the illumination wavelength was 0.5 μm.

The membrane's surface roughness was set by a random function with a uniform distribution, and the roughness parameter Ra was selected from the range 0.1–20 μm.

To check the effect of the diaphragm radius on the speckle size, the image intensity of the membrane with the roughness parameter Ra = 20 μm was calculated using formula (11) with a deflection arrow of 0.2 μm and various aperture radii. As is seen from Fig. 3, the size of speckle structures decreases with increasing aperture size.

To estimate the error of phase reconstruction from speckle interferograms, it was first necessary to learn how to synthesise these interferograms. Speckle interferograms were calculated according to formula (13), which describes the coherent addition of a wave field reflected from the object, a field passed through the optical system, and a plane wave directed

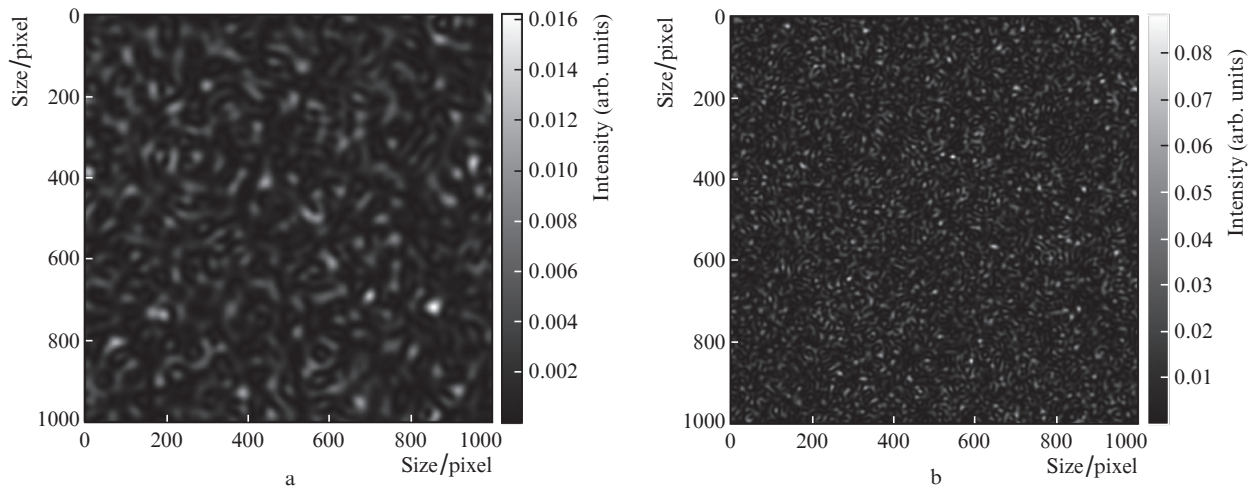

Figure 3. Membrane images with a roughness parameter Ra = 20 μm, obtained using a coherent optical system with aperture radii of (a) 20 and (b) 50 pixels.

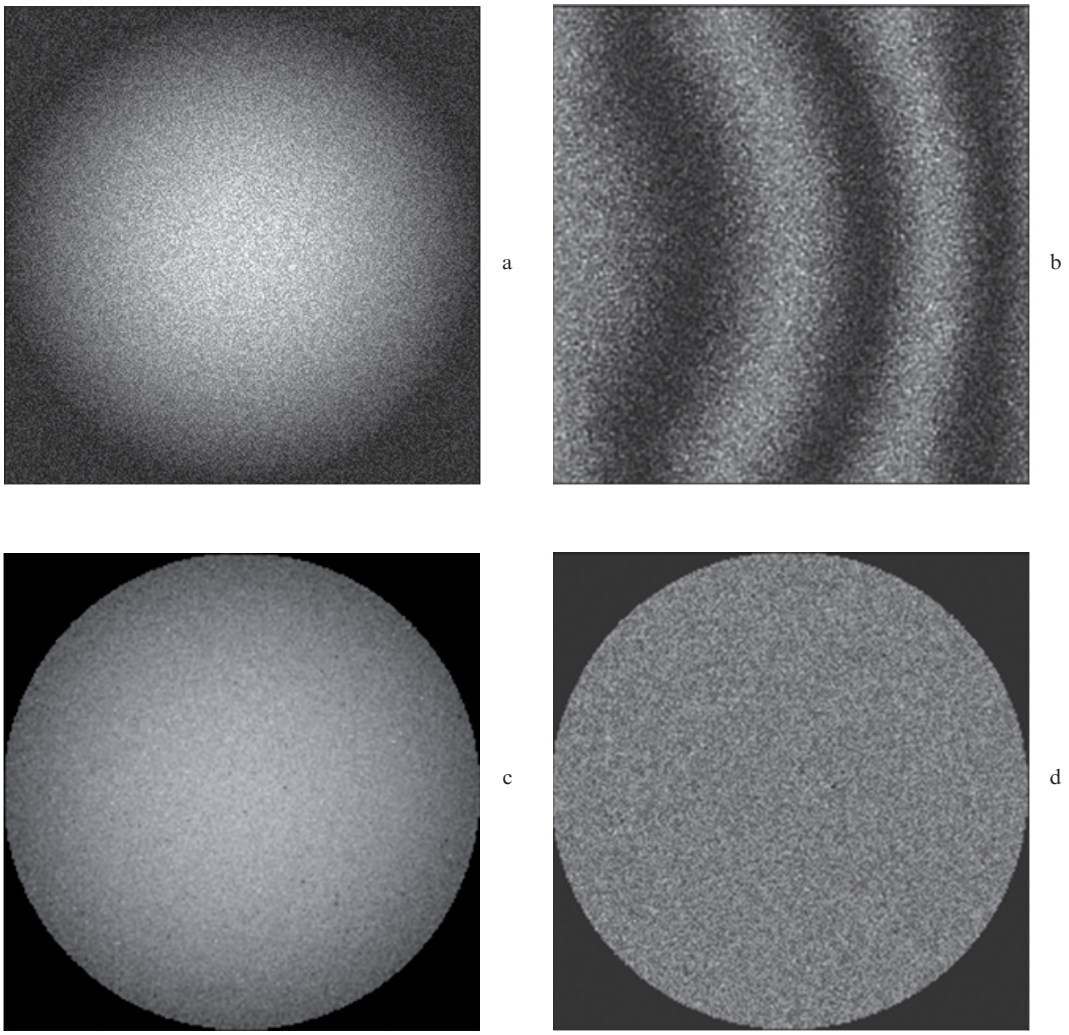

Figure 4. (a) Membrane topogram, (b) image of the membrane's speckle interferogram, (c) result of membrane topogram reconstruction and (d) field of reconstruction errors with a deflection arrow of 1.0 μm.

at an angle to the recording plane with subsequent quadratic recording.

The initial simulation was aimed at clarifying the choice of the angle between the object and reference beams, since it

determines the number of interferogram fringes. A large angle leads to an increase in the number of fringes that can no longer be resolved by the optical system.

The simulation has shown that, when the angle between the interfering beams is equal to 1°, there is no more than five fringes on the interferogram. The simulation results also show that contrasting interference fringes on the speckle interferogram are possible if the membrane roughness parameter is less than the radiation wavelength used.

In this regard, a membrane with a roughness of Ra = 0.1 μm, which is less than the wavelength of 0.5 μm, was selected for further simulation, while the angle between the interfering beams amounted to 1° with the aperture radius of 100 pixels.

Next, a study was conducted to reconstruct the membrane topogram from a set of five synthesised speckle interferograms using the phase-shift technique described above. Figure 4 shows the results of this study and presents the initial topogram of the deformed membrane in the form of a spherical segment with a deflection arrow of 1.0 μm, one of synthesised speckle interferograms, the result of reconstructing the topogram of the membrane's rough surface, and a two-dimensional map of the difference between the reconstructed and original topograms. In fact, this difference is a plane, but there are deviations from it due to the presence of noise. Therefore, the measure of the reconstruction error is the root mean square (rms) deviation of this difference from the plane, amounting to 0.08 μm.

Using the developed mathematical model, computational experiments were performed to evaluate the rms deviation of the result of the membrane topogram reconstruction at different values of the deflection arrow, i.e. at different strains. As can be seen from Fig. 5, the reconstruction error increases with an increase in the deflection arrow, which is associated with an increase in the gradient at the edge (Fig. 5c) and, as a result, with a decrease in the capability of resolving the interference fringes by the video camera matrix.

Thus, we obtained the dependence of the reconstruction error on the strain of an elastic rough membrane in the optical 4*f* scheme using the phase-shift algorithm, which implies that the upper limit of the range of possible strains does not exceed 12 μm.

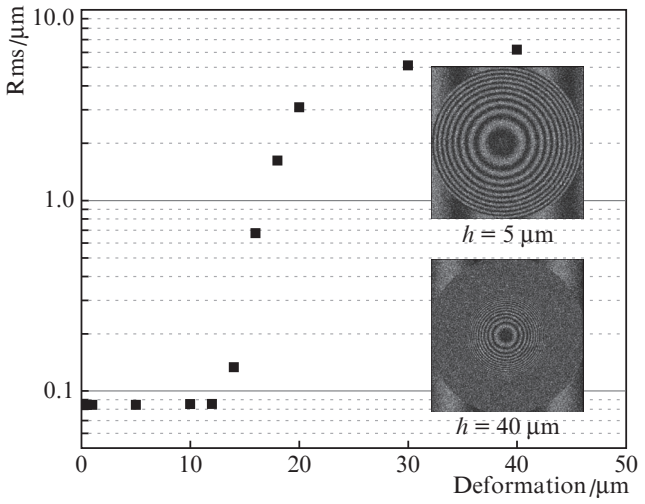

Figure 5. Dependence of rms deviation of the topogram reconstruction result on the strain value. The insets show speckle interferograms of the test object under strains of 5 and 40 μm.

4. Simulation of the object strain and obtaining of a shearogram

This section describes the results of computer simulation of speckle-shearing interferometry (shearography). A computer model (CM) of the object was developed, which was necessary for subsequent simulation of the process of measuring the stress–strain states using digital shearography.

The purpose of the computer simulation itself was to compare the simulation results with experimental measurements of the strain of a physical object having the same parameters as the computer model, and to evaluate the accuracy of such measurements.

The main requirement for the choice of the CM is that it should allow one, using the known formulas of the theory of strength of materials, to calculate the displacement field in the course of deformation. An elastic circular membrane rigidly attached around its circumference to the base may serve as such a model (Fig. 6). A concentrated force is applied along the normal to the membrane surface at its centre on the back side, under the action of which the membrane surface's points undergo micro-displacements, the field of which is the subject of research.

In some monographs [16, 17], the displacement field for such a model is described by the formula

$$W(R) = \frac{F}{16\pi D}\left[(a^2 - R^2) + 2R^2 \ln\left(\frac{R}{a}\right)\right], \qquad (14)$$

where W is the displacement along the normal (z axis) to the membrane surface; F is the applied force; D is the membrane stiffness; a is the membrane radius; and R is the distance from the membrane centre.

A computer version of this model was developed and used to simulate the process of stress–strain state measurements. Speckle interferograms of the CM of this test object, synthesised according to the technique described in Section 3, served as initial data for this simulation. First, the object topogram was reconstructed for a certain load from the original speckle interferograms, and then the displacement field gradient was determined as the difference between two topograms shifted relative to each other. The practical significance of this simulation is that it allows one to pre-set the necessary image shift value in the shearograph to adjust its sensitivity.

To compare the results of computer simulation with experimental data, a calibration device was developed and manufactured, described in our paper [18] and used to calibrate a shearograph prototype developed at the Federal State Unitary Enterprise VNIIOFI. This device is a rough circular membrane attached to a massive base around the circumference by means of screws (Fig. 6), it has standardised metrological characteristics and represents a working standard of strain.

A concentrated force is applied along the normal to the membrane surface at its centre on the back side, under the impact of which the membrane experiences bending strains. The magnitude of the displacement of the force application point was measured using a 01IMPTs indicator head with an error of ± 0.3 μm.

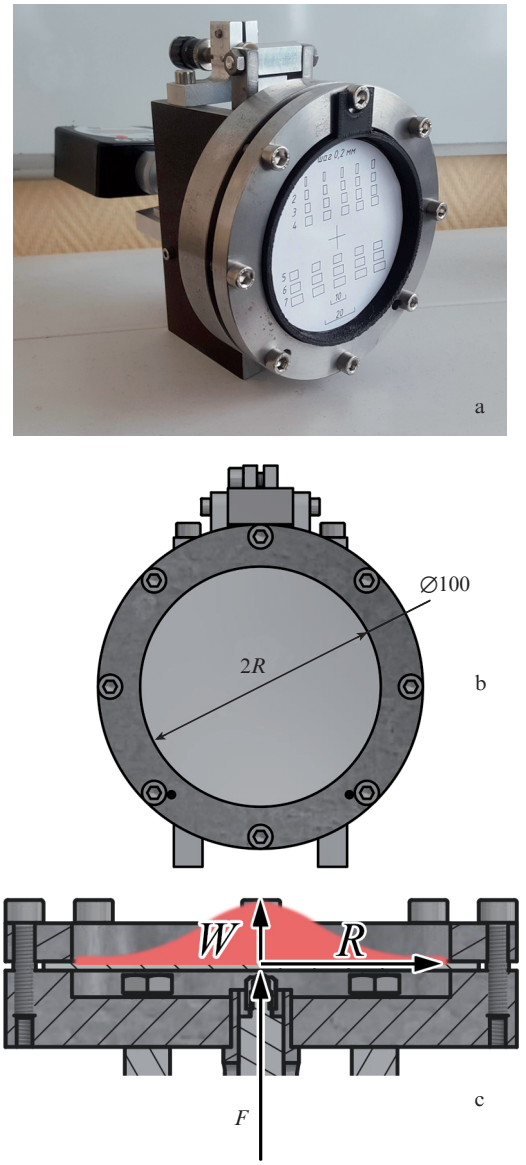

Figure 6. (a) Calibration device, (b) membrane (front view), and (c) cross-section view of the calibration device.

An experimental study of the membrane strain in the calibration device was performed on the shearograph prototype, the external appearance of which is shown in Fig. 7.

A laser with a wavelength $\lambda = 532$ nm was used as a radiation source. The camera's viewing angle and illumination angle ensured the shooting of a membrane with a diameter of 100 mm.

A half-tone image of the reconstructed membrane displacement field obtained by computer simulation and a similar experimental image are shown in Fig. 8. The membrane strain (according to the indicator) was 1 μm.

Figure 7. Experimental prototype of the shearograph.

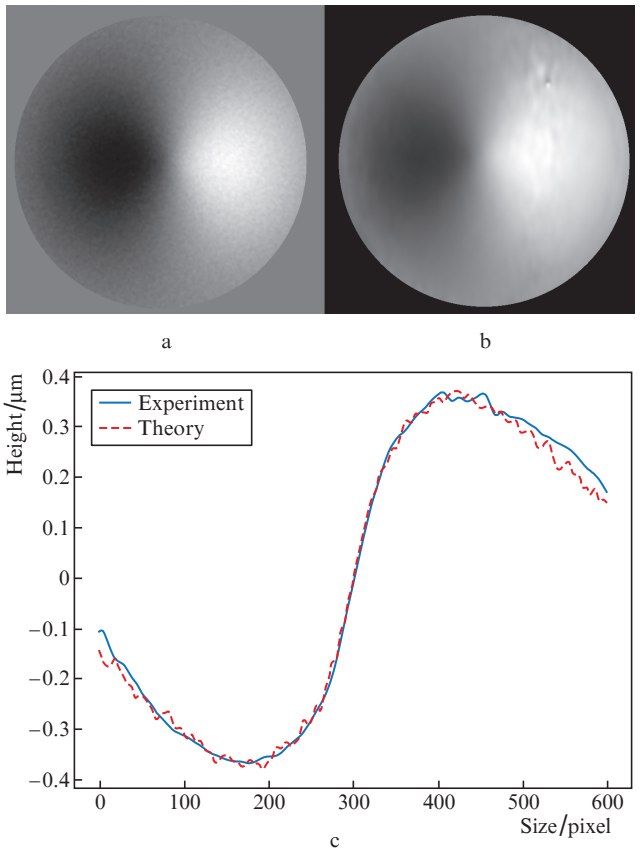

Figure 8. (a) Theoretical and (b) experimental shearograms, as well as (c) cross-section profiles of shearograms.

The results of a physical and computer experiment were compared with respect to the central horizontal cross sections of these images. The rms deviation of the difference between them, which amounted to 0.02 μm, served as the comparison criterion for these data.

5. Conclusions

We have developed a computer (virtual) model of a test object and the speckle interferometer's optical scheme, which is essentially its digital twin. The simulation and experimental results are shown to be in a good agreement. The presented method of numerical simulation makes it possible to set any objects, including ideal ones, to verify the system operation. This approach allows one to improve the algorithms and optimise the optical scheme to obtain accurate results of the stress–strain state measurements. The developed model enables us to predict the result of the speckle interferometer operation with objects having various parameters. This computer model is a 'digital standard' and can be used to evaluate the metrological characteristics of measuring instruments. Its further improvement will make it possible to avoid using the

material standard in the measurement process using the method of shearing speckle interferometry.

Acknowledgements. This work was carried out using the equipment of the Shared Use Equipment Center for high-precision measuring in photonics (ckp.vniiofi.ru, VNIIOFI) and supported by the Ministry of Science and Higher Education of the Russian Federation (Agreement No. 05.595.21.0005, unique identifier RFMEFI59519X0005).

References

1. Schars U., Jueptner W. *Digital Holography. Digital Hologram Recording, Numerical Reconstruction, and Related Techniques* (Berlin–Heidelberg–New York: Springer-Verlag, 2005).
2. Steinchen W., Yang L. *Digital Shearography: Theory and Application of Digital Speckle Pattern Shearing Interferometry* (SPIE Press, 2003).
3. Zhao Q., Dan X., Sun F., et al. *Appl. Sci.*, **8**, 2662 (2018).
4. Xiea X., Yang L., Chena X., Xua N., Wang Y. *Proc. SPIE*, **8916**, 89160D-1 (2013).
5. Xie X., Yang L., Xu N., Chen X. *Appl. Opt.*, **52**, 4063 (2013).
6. Hariharan P., Oreb B.F., Eiju T. *Appl. Opt.*, **26**, 2504 (1987).
7. Malacara D., Servin M., Malacara Z. *Interferogram Analysis for Optical Testing* (Boca Raton: CRC Press, 2005).
8. Waldner S.P. *PhD Thesis* (Zurich, 2000).
9. West C.M. *Holographic Interferometry* (New York: Wiley, 1979; Moscow: Mir, 1982).
10. Badalyan N.P., Kiiko V.V., Kislov V.I., Kozlov A.B. *Quantum Electron.*, **38**, 477 (2008) [*Kvantovaya Elektron.*, **38**, 477 (2008)].
11. Mysina N.Yu., Maksimova L.A., Gorbatenko B.B., Ryabukho V.P. *Quantum Electron.*, **45**, 979 (2015) [*Kvantovaya Elektron.*, **45**, 979 (2015)].
12. Guzhov V.I., Turuntaev D.A. *Avtometriya*, **5**, 116 (2000).
13. Song L., Zhou Z., et al. *Opt. Express,* **7**, 798 (2016).
14. Savonin S.A. *Cand. Thesis* (Saratov, 2016).
15. Goodman W. *Introduction to Fourier Optics* (New York: McGraw-Hill, 1968; Moscow: Mir, 1970).
16. Birger I.A. *Raschet na prochnost' detaley mashin* (Strength Analysis of Machine Parts) (Moscow: Mashinostroenie, 1959).
17. Bazhanov V. L. et al. *Raschet konstruktsiy na teplovyye vozdeystviya* (Calculation of Structures for Thermal Effects) (Moscow: Mashinostroenie, 1969).
18. Ivanov A.D., Minaev V.L., Vishnyakov G.N., et al. *Meas. Tech.*, **62**, 795 (2019).